

New Test Beam Results of 3D and Pad Detectors Constructed with Poly-Crystalline CVD Diamond

M. Reichmann^{z,*}, A. Alexopoulos^c, M. Artuso^l, F. Bachmair^x, L. Bäni^x, M. Bartosik^c, J. Beacham^m, H. Beck^w, V. Bellini^b, V. Belyaev^l, B. Bentele^s, P. Bergonzo^k, A. Bes^{aa}, J.-M. Brom^g, M. Bruzzi^d, G. Chiodini^z, D. Chren^f, V. Cindroⁱ, G. Claus^g, J. Collot^{aa}, J. Cumalat^s, A. Dabrowski^c, R. D'Alessandro^d, D. Dauvergne^{aa}, W. de Boer^j, S. Dick^m, C. Dorfer^x, M. Dünser^c, G. Eigen^{ad}, V. Eremin^f, J. Forneris^o, L. Gallin-Martel^{aa}, M.L. Gallin-Martel^{aa}, K.K. Gan^m, M. Gastal^c, C. Giroletti^q, M. Goffe^g, J. Goldstein^q, A. Golubev^h, A. Gorišekⁱ, E. Grigoriev^h, J. Grosse-Knetter^w, A. Grummer^u, M. Guthoff^c, B. Hitiⁱ, D. Hits^x, M. Hoferkamp^u, T. Hofmann^c, J. Hosslet^g, J.-Y. Hostachy^{aa}, F. Hügging^a, C. Hutton^q, J. Janssen^a, H. Kagan^m, K. Kanxheri^{ab}, R. Kass^m, M. Kis^e, G. Krambergerⁱ, S. Kuleshov^h, A. Lacoste^{aa}, S. Lagomarsino^d, A. Lo Giudice^o, E. Lukosi^y, C. Maazouzi^g, I. Mandicⁱ, A. Marino^s, C. Mathieu^g, M. Menichelli^{ab}, M. Mikužⁱ, A. Morozzi^{ab}, J. Moss^{ac}, R. Mountain^l, S. Murphy^v, M. Muškinjaⁱ, A. Oh^v, P. Oliviero^o, D. Passeri^{ab}, H. Pernegger^c, R. Perrino^z, F. Picollo^o, M. Pomorski^k, R. Potenza^b, A. Quadt^w, F. Rarbi^{aa}, A. Re^o, G. Riley^{ab}, S. Roe^c, D.A. Sanz-Becerra^x, M. Scaringella^d, D. Schaefer^c, C.J. Schmidt^e, E. Schioppa^c, S. Schnetzerⁿ, S. Sciortino^d, A. Scorzoni^{ab}, S. Seidel^u, L. Servoli^{ab}, D.S. Smith^m, B. Sopko^r, V. Sopko^f, S. Spagnolo^z, S. Spanier^y, K. Stenson^s, R. Stoneⁿ, B. Stugo^{ad}, C. Sutura^b, M. Traeger^e, D. Tromson^k, W. Trischuk^p, C. Tuve^b, J. Velthuis^q, N. Venturi^c, E. Vittone^o, S. Wagner^s, R. Wallny^x, J.C. Wang^t, C. Weiss^c, N. Wermes^a, M. Yamouni^{aa}, M. Zalieckas^{ad}, M. Zavrtanikⁱ

^aUniversität Bonn, Bonn, Germany, ^bINFN/University of Catania, Catania, Italy, ^cCERN, Geneva, Switzerland, ^dINFN/University of Florence, Florence, Italy, ^eGSI, Darmstadt, Germany, ^fIoffe Institute, St. Petersburg, Russia, ^gIPHC, Strasbourg, France, ^hITEP, Moscow, Russia, ⁱJožef Stefan Institute, Ljubljana, Slovenia, ^jUniversität Karlsruhe, Karlsruhe, Germany, ^kCEA-LIST Technologies Avancees, Saclay, France, ^lMEPHI Institute, Moscow, Russia, ^mThe Ohio State University, Columbus, OH, USA, ⁿRutgers University, Piscataway, NJ, USA, ^oUniversity of Torino, Torino, Italy, ^pUniversity of Toronto, Toronto, ON, Canada, ^qUniversity of Bristol, Bristol, UK, ^rCzech Technical University, Prague, Czech Republic, ^sUniversity of Colorado, Boulder, CO, USA, ^tSyracuse University, Syracuse, NY, USA, ^uUniversity of New Mexico, Albuquerque, NM, USA, ^vUniversity of Manchester, Manchester, UK, ^wUniversität Göttingen, Göttingen, Germany, ^xETH Zürich, Zürich, Switzerland, ^yUniversity of Tennessee, Knoxville, TN, USA, ^zINFN-Lecce, Lecce, Italy, ^{aa}LPSC-Grenoble, Grenoble, France, ^{ab}INFN-Perugia, Perugia, Italy, ^{ac}California State University, Sacramento, CA, USA, ^{ad}University of Bergen, Bergen, Norway,

Abstract

Chemical Vapour Deposition (CVD) diamond is possible material for particle detectors in a harsh radiation environment. This article is discussing beam test results of 3D pixel detectors fabricated with poly-crystalline CVD diamonds. The cells of the devices have a size of $50\mu\text{m} \times 50\mu\text{m}$ with columns $2.6\mu\text{m}$ in diameter. The cells were ganged in a 3×2 and a 5×1 pattern to match the layouts of the pixel read-out chips currently used in the CMS and ATLAS experiments at the Large Hadron Collider, respectively. In beam tests, using tracks reconstructed with a high precision tracking telescope, both devices achieved tracking efficiencies greater than 97 %. The efficiency of both devices plateaus at a bias voltage of 30 V. The latest high rate beam test results of irradiated poly-crystalline CVD diamond pad detectors are also presented. In measurements with particle fluxes up to 20 MHz/cm^2 and irradiations up to $8 \cdot 10^{15}\text{ n/cm}^2$ it could be shown that the pulse height of irradiated poly-crystalline CVD diamonds does not depend on flux to the $O(2\%)$.

Keywords: Diamond Detectors, 3D Sensors, Particle Flux

1. Introduction

The radiation levels of the High-Luminosity Large Hadron Collider (HL-LHC) will become a big challenge for the future detectors. By 2028 an instantaneous luminosity of $7.5 \cdot 10^{34}\text{ cm}^{-2}\text{ s}^{-1}$ is and total dose of the $O(10\text{ MGy})$ are expected [1]. In this environment the innermost tracking layer at a transverse distance of $\sim 30\text{ mm}$ to the interaction point is expected to be exposed to a total fluence of $2 \cdot 10^{16}\text{ n}_{\text{eq}}/\text{cm}^2$ [2]. The lifetime of the current planar silicon tracking detectors is expected to be about one year in the HL-LHC.

After a large fluence, all detector materials become trap limited with a mean drift distance below $75\mu\text{m}$. Due to its properties, such as the displacement energy of 42 eV/atom and the band gap of 5.5 eV , the RD42 collaboration is investigating CVD diamond as a possible detector material [3]. In various studies it was shown that compared to corresponding silicon detectors, diamond is at a minimum three times more radiation hard [4], collecting the charges at least two times faster [5] and conducting heat four times more efficiently [6].

By now the technology of diamond detectors is well established in high energy physics. Many high energy physics experiments are already using Beam Condition Monitors or Beam Loss Monitors based on CVD diamonds [7], [8], [9].

The RD42 collaboration is also investigating a novel detector

*Corresponding author

design, namely 3D detectors. This concept is a possible way to reduce the drift distance below the mean drift distance of an irradiated sensor without reducing the total number of the excited electron-hole pairs.

Also the particle flux of the HL-LHC will be in a completely new regime. Hence high rate studies of pad detectors were performed at Paul Scherrer Institut (PSI) with nearly minimum ionising particles (MIPs) and tunable particle fluxes up to $O(20 \text{ MHz/cm}^2)$.

2. 3D Pixel Detectors

By placing the column like electrodes inside the detector material, the 3D geometry reduces the drift distance of the charge carriers created by ionising particles compared to a planar device. More details about the working principle can be found in [10], [11]. All devices discussed in the following were built on poly-crystalline CVD (pCVD) diamond.

2.1. Fabrication

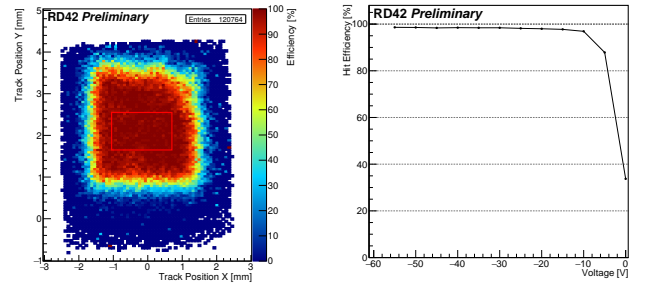
In order to generate the electrodes in diamond, columns are drilled using a 130 fs laser with a wavelength of 800 nm which converts the diamond into a electrically conductive mixture of different carbon phases [12]. The conductivity of the columns is of the $O(1 (\Omega\text{cm})^{-1})$. By applying Spatial Light Modulation (SLM) a column yield of $>99\%$ and a column diameter of $2.6 \mu\text{m}$ can be achieved [13]. The largest fabricated device has about 4000 3D cells, where one cell consists out of four bias electrodes and one read-out electrode in the centre.

The detector is built by connecting to the bias and readout columns with surface metallisation and bump bonding the sensor to the readout electronics as shown in Figure 1. For the detectors described in here a cell size of $50 \mu\text{m} \times 50 \mu\text{m}$ was chosen. Since the layout of the available readout chips (ROCs) has a different pixel pitch several cells had to be ganged together.

2.2. PSI46digV2.1respin read-out

The first prototype of a $50 \mu\text{m} \times 50 \mu\text{m}$ 3D pixel detector was connected to the PSI46digV2.1respin ROC [14] with a 3×2 cell ganging to match the pixel pitch of $150 \mu\text{m} \times 100 \mu\text{m}$. The 3D sensors were bump bonded to the ROC at the Nanofabrication Lab in Princeton with indium bumps by putting equal height indium columns on both ROC and the sensor and then pressing them together. The preliminary beam test results show that relative to a planar silicon device the efficiency in the fiducial area amounts to 99.3% (Figure 2a). This efficiency estimation does not account for non-working 3D cells in this region which can happen due to broken or missing columns or due to metalisation issues. In order to acquire this information further data has to be analysed. Nevertheless, a small mismatch between a 3D and a planar device is expected due to regions inside of the detector where the electric field is low [15] and the

columns themselves. Figure 2b shows that the device already plateaus at a voltage of 30 V. The preliminary analysis of the pulse height distribution yields a mean value of $\sim 11 \text{ ke}$. The up-



(a) 3×2 efficiency. The red box marks the fiducial area. (b) Efficiency vs. voltage.

Figure 2: 3×2 results.

dated pulse height information will be reported after the precise pulse height calibration of the ROC is performed.

2.3. FE-I4b read-out

The second prototype was connected to the FE-I4b ROC [16]

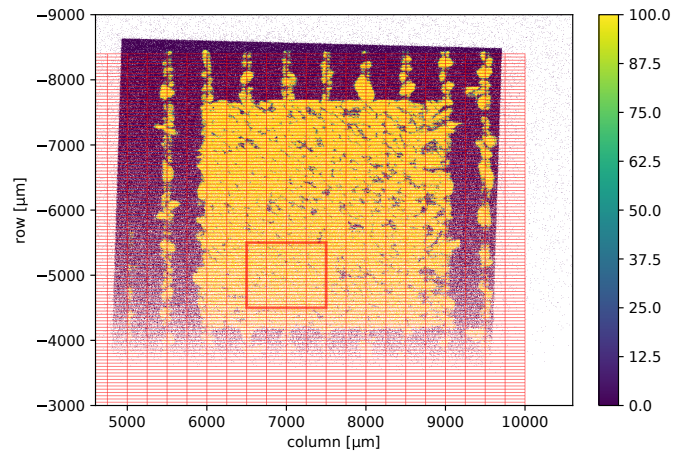


Figure 3: 5×1 efficiency. The red box denotes the fiducial area.

with a 5×1 cell ganging due to its pitch of $250 \mu\text{m} \times 50 \mu\text{m}$. The bump bonding was performed at IFAE-CNM in Barcelona by an adapted process with tin-silver bumps. Using a high resolution beam telescope with a spatial resolution of $3 \mu\text{m}$ at the device under test the efficiency could be mapped to the spatial coordinates. The results yield an efficiency of 97.8% in the contiguous fiducial area (Figure 3). The low efficiency is most likely due to issues with the bump bonding or the metallisation. The preliminary pulse height in the fiducial region amounts to $\sim 15 \text{ ke}$ which is consistent with the result of the first prototype considering the different momenta of the incident particles. An updated pulse height will be reported as soon as the precise pulse height calibration for this ROC is performed.

3. High Rate Studies

The HL-LHC will reach particle fluxes of $O(\text{GHz}/\text{cm}^2)$ hence it is very important to understand the effect of the incident particle flux on the signal of pCVD diamonds. In order to conduct such a study it is essential to be able to vary the particle flux over a large range. The πM1 beam line at the High Intensity Proton Accelerator (HIPA) at PSI [17] can provide beams with continuously tunable fluxes from the order of $1 \text{ kHz}/\text{cm}^2$ up to $20 \text{ MHz}/\text{cm}^2$. The πM1 beam is bunched with a spacing of 19.7 ns . For these studies a π^+ beam with a momentum of $260 \text{ MeV}/c$ was chosen in order to reach the highest possible flux [18]. In total 17 pCVD diamonds were measured.

3.1. Setup

The planar diamond sensors were connected in a pad geometry and prepared as described in [19]. In order to resolve individual particles at high particle rates the sensors were connected to a fast, amplifier with low electronic noise and a rise time of approximately 5 ns . The resulting waveforms were digitised and recorded in a beam telescope setup which provides spatial information of the hits in the diamond detector. Due to the low momentum of the incident particles the spatial resolution of the telescope is of the $O(100 \mu\text{m})$.

3.2. Results

pCVD diamond has an interior crystal structure where the individual grains have slightly different properties. Therefore the size of the measured signal in pCVD depends also on the spatial position as can be seen in Figure 4. However this behaviour is constant and neither depends on time nor on rate.

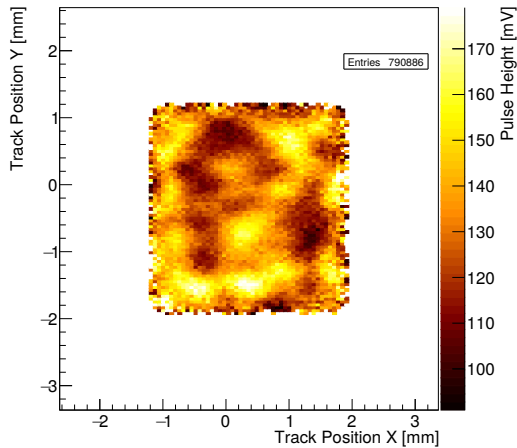


Figure 4: Pulse height map of a pCVD diamond.

As an important factor also the beam induced current is studied depending on the particle rate. In 80 % of the measured diamonds the current is proportional to the flux and the leakage current without a beam is of the $O(1 \text{ nA})$. The other 20 % of the diamonds show shifting base lines or erratic currents [20]. These diamonds are not shown in this article.

In order to measure the signal behaviour as a function of incident particle flux and irradiation, several rate scans with both

polarities of the bias voltage were performed. Figure 5 shows the final results for a pCVD diamond with various fluences

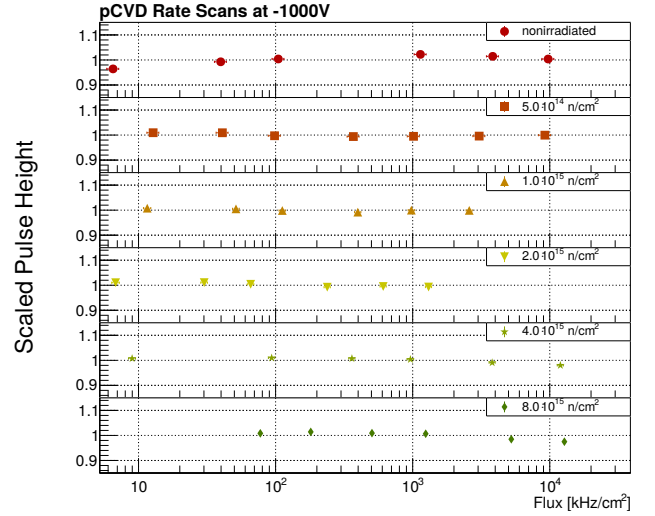


Figure 5: Pulse height versus incident particle flux for a pCVD diamond for various fluences at -1000 V .

up to a maximum particle flux of $20 \text{ MHz}/\text{cm}^2$. The sensors were irradiated at the irradiation facilities at the JSI TRIGA reactor in Ljubljana with fast reactor neutrons in steps up to $8 \cdot 10^{15} \text{ n}/\text{cm}^2$ [21]. The mean pulse height of the single scans is scaled to 1. The pulse height is flat with respect to the flux deviating less than 2 % from the mean.

We also observed a single diamond with a large rate dependence losing 90 % of the signal at highest rate. After the surface was cleaned and processed with Reactive Ion Etching (RIE), the device was reprocessed. A new measurement showed a deviation of less than 2 % from the mean pulse height. This leads us to the conclusion that this rate effect is due to surface properties and is possible to repair.

4. Conclusion

There is progress in the development of radiation tolerant particle detectors based on pCVD diamonds. The working principle of 3D pixel detectors was proven down to cell sizes of $50 \mu\text{m} \times 50 \mu\text{m}$ and column diameters of $2.6 \mu\text{m}$. The largest device has a number of 4000 cells and the efficiency of the column drilling process is now above 99 %. The first prototypes of small cell 3D pixel detectors read out more charge than any planar pCVD diamond detector. The measured relative hit efficiency of the 3D pixel detectors reaches 99.3 % compared to a silicon device.

It was found that irradiated pCVD diamond detectors work reliably and show no signal dependence to the $O(2 \%)$ up to an incident particle flux of $20 \text{ MHz}/\text{cm}^2$. This was shown for an irradiation up to a fluence of $8 \cdot 10^{15} \text{ n}/\text{cm}^2$. The beam induced current of a pCVD diamond is proportional to the flux and the leakage current is of the $O(1 \text{ nA})$. A small fraction of the diamonds shows a large rate dependence which is most likely to surface issues and is possible to correct.

Acknowledgements

We want to thank the laser team in Oxford around Patrick Salter for providing us with these great 3D detectors. Further-
more we want to thank Bert Harrop in Princeton and the team at IFAE for bump bonding our devices.

The research leading to these results received funding from the European Union's Horizon 2020 research and innovation program under grant agreement No. 654168. This work was also partially supported by the Swiss National Science Foundation grant #20FL20_154216, ETH grant 51 15-1, Royal Society Grant UF120106, the U.S. Department of Energy through grant DE-SC0010061, the UK Science and Technology Facilities Council ST/P002846/1 and the Swiss Government Excellence Scholarship ESKAS No. 2015.0808.

References

- Contardo D, Klute M, Mans J, Silvestris L, Butler J. Technical Proposal for the Phase-II Upgrade of the CMS Detector. Tech. Rep. CERN-LHCC-2015-010. LHCC-P-008. CMS-TDR-15-02; Geneva; 2015. URL: <http://cds.cern.ch/record/2020886>.
- Auzinger G (CMS Collaboration). Upgrade of the CMS Tracker for the High Luminosity LHC. Tech. Rep. CMS-CR-2016-268; CERN; Geneva; 2016. URL: <https://cds.cern.ch/record/2227193>.
- Kagan H, Trischuk W. Development of Diamond Tracking Detectors for High Luminosity Experiments at the LHC, HL-LHC and Beyond. Tech. Rep. CERN-LHCC-2018-015. LHCC-SR-005; CERN; Geneva; 2018. URL: <https://cds.cern.ch/record/2320382>.
- de Boer W, Bol J, Furgeri A, Miller S, Sander C, Berdermann E, Pomorski M, Huhtinen M. Radiation hardness of diamond and silicon sensors compared. *physica status solidi (a)* 2007;204(9):3004–10. URL: <http://dx.doi.org/10.1002/pssa.200776327>. doi:10.1002/pssa.200776327.
- Pernegger H, Eremin V, Fraiss-Klbi H, Griesmayer E, Kagan H, Roe S, Schnetzer S, Stone R, Trischuk W, Twitchen D, Weilhammer P, Whitehead A. Charge-carrier properties in synthetic single-crystal diamond measured with the transient-current technique. *J Appl Phys* 2005;97(7):73704–1. URL: <https://cds.cern.ch/record/909063>.
- Zhao S. Characterization of the electrical properties of polycrystalline diamond films. Ph.D. thesis; The Ohio State University; 1994. URL: <http://wwwlib.umi.com/dissertations/fullcit?p9421043>.
- Edwards AJ, Brau B, Bruinsma M, Burchat P, Kagan H, Kass R, Kirkby D, Petersen BA, Zoeller M. Radiation monitoring with diamond sensors in babar. *IEEE Transactions on Nuclear Science* 2004;51(4):1808–11. doi:10.1109/TNS.2004.832634.
- Eusebi R, Wallny R, Tesarek R, Dong P, Sfyrila A, Trischuk W, Schrupp C. A diamond-based beam condition monitor for the cdf experiment. 2006;709–12. doi:10.1109/NSSMIC.2006.355953.
- Schaefer D. The ATLAS Diamond Beam Monitor: luminosity Detector on the LHC. Tech. Rep. ATL-INDET-PROC-2015-009; CERN; Geneva; 2015. URL: <https://cds.cern.ch/record/2034225>.
- Parker S, Kenney C, Segal J. 3D - A proposed new architecture for solid-state radiation detectors. *Nuclear Instruments and Methods in Physics Research Section A: Accelerators, Spectrometers, Detectors and Associated Equipment* 1997;395(3):328–43. URL: <http://www.sciencedirect.com/science/article/pii/S0168900297006943>. doi:[https://doi.org/10.1016/S0168-9002\(97\)00694-3](https://doi.org/10.1016/S0168-9002(97)00694-3); proceedings of the Third International Workshop on Semiconductor Pixel Detectors for Particles and X-rays.
- Bachmair F, Bni L, Bergonzo P, Caylar B, Forcolin G, Haughton I, Hits D, Kagan H, Kass R, Li L, Oh A, Phan S, Pomorski M, Smith D, Tyzhnevyy V, Wallny R, Whitehead D. A 3D diamond detector for particle tracking. *Nuclear Instruments and Methods in Physics Research Section A: Accelerators, Spectrometers, Detectors and Associated Equipment* 2015;786:97–104. URL: <http://www.sciencedirect.com/science/article/pii/S0168900215003496>. doi:<https://doi.org/10.1016/j.nima.2015.03.033>.
- Kononenko T, Komlenok M, Pashinin V, Pimenov S, Konov V, Neff M, Romano V, Lthy W. Femtosecond laser microstructuring in the bulk of diamond. *Diamond and Related Materials* 2009;18(2):196–9. URL: <http://www.sciencedirect.com/science/article/pii/S0925963508003981>. doi:<https://doi.org/10.1016/j.diamond.2008.07.014>; nDNC 2008 Proceedings of the International Conference on New Diamond and Nano Carbons 2008.
- Sun B, Salter PS, Booth MJ. High conductivity micro-wires in diamond following arbitrary paths. *Applied Physics Letters* 2014;105(23):231105. URL: <https://doi.org/10.1063/1.4902998>. doi:10.1063/1.4902998. arXiv:<https://doi.org/10.1063/1.4902998>.
- Kornmayer A, Miller T, Husemann U. Studies on the response behaviour of pixel detector prototypes at high collision rates for the CMS experiment. 2015. URL: <https://cds.cern.ch/record/2264667>; presented 04 Dec 2015.
- Forcolin GT, Oh A, Da Via C. Development and simulation of 3D diamond detectors. 2018. URL: <https://cds.cern.ch/record/2636028>; presented 2018.
- Garcia-Sciveres M, Arutinov D, Barbero M, Beccherle R, Dube S, Elledge D, Fleury J, Fougeron D, Gensolen F, Gnani D, Gromov V, Hemptek T, Karagounis M, Kluit R, Kruth A, Mekkaoui A, Menouni M, Schipper J. The FE-I4 Pixel Readout Integrated Circuit. Tech. Rep. ATL-UPGRADE-PROC-2010-001; CERN; Geneva; 2010. URL: <https://cds.cern.ch/record/1231359>.
- PSI. High Intensity Proton Accelerator at PSI. <https://www.psi.ch/rf/hipa>; 2017.
- PSI. Pion and electron fluxes in piM1. <http://aea.web.psi.ch/beam2lines/pim1c.html>; 2015.
- Wallny R, et al. (RD42). Beam test results of the dependence of signal size on incident particle flux in diamond pixel and pad detectors. *JINST* 2015;10(07):C07009. URL: <https://cds.cern.ch/record/2159123>.
- Mikuz M, Cindro V, Dolenc I, Kagan H, Kramberger G, Fraiss-Kolbl H, Gorisek A, Griesmayer E, Macek B, Mandic I, Niegl M, Pernegger H, Smith D, Tardif D, Trischuk W, Weilhammer P, Zavrtanik M. The atlas beam conditions monitor. vol. 3. ISBN 978-1-4244-0922-8; 2008:1914–7. doi:10.1109/NSSMIC.2007.4436530.
- Snoj L, Åerovnik G, Trkov A. Computational analysis of irradiation facilities at the jsi triga reactor. *Applied Radiation and Isotopes* 2012;70(3):483–8. URL: <http://www.sciencedirect.com/science/article/pii/S0969804311005963>. doi:<https://doi.org/10.1016/j.apradiso.2011.11.042>.